

Enhancing Diabetic Retinopathy Detection Through Machine Learning with Restricted Boltzmann Machines

Dr. Venkateswara Rao Naramala¹, B.Anjanees Kumar², Dr. Vuda Sreenivasa Rao³, Dr. Annapurna Mishra⁴,
Shaikh Abdul Hannan⁵, Prof. Ts. Dr. Yousef A. Baker El-Ebiary⁶, R. Manikandan⁷

Professor, CSE (AI&ML), RVR & JC College of Engineering, Chowdavaram, Guntur, Andhra Pradesh¹
Associate Professor, Electronics and Communication Engineering, Dadi Institute of Engineering and Technology,
Anakapalle, Andhra Pradesh, India²

Associate Professor, Department of CSE, Koneru Lakshmaiah Education Foundation, Vaddeswaram, AP, India³
Associate Professor, Electronics and Communication Engineering, Silicon Institute of Technology,
Bhubaneswar, India, Pincode: 7510244

Assistant Professor, Department of Computer Science and Information Technology, Albaha University,
Albaha, Kingdom of Saudi Arabia⁵

Professor, Faculty of Informatics and Computing, UniSZA University, Malaysia⁶.
Research Scholar, Vel Tech Rangarajan Dr. Sagunthala R&D Institute of Science and Technology,
Avadi, Chennai, Tamil Nadu, India-600062⁷

Abstract—Diabetes is a potentially sight-threatening condition that can lead to blindness if left undetected. Timely diagnosis of diabetic retinopathy, a persistent eye ailment, is critical to prevent irreversible vision loss. However, the traditional method of diagnosing diabetic retinopathy through retinal testing by ophthalmologists is labor-intensive and time-consuming. Additionally, early identification of glaucoma, indicated by the Cup-to-Disc Ratio (CDR), is vital to prevent vision impairment, yet its subtle initial symptoms make timely detection challenging. This research addresses these diagnostic challenges by leveraging machine learning and deep learning techniques. In particular, the study introduces the application of Restricted Boltzmann Machines (RBM) to the domain. By extracting and analyzing multiple features from retinal images, the proposed model aims to accurately categorize anomalies and automate the diagnostic process. The investigation further advances with the utilization of a U-network model for optic segmentation and employs the Squirrel Search Algorithm (SSA) to fine-tune RBM hyperparameters for optimal performance. The experimental evaluation conducted on the RIM-ONE DL dataset demonstrates the efficacy of the proposed methodology. A comprehensive comparison of results against previous prediction models is carried out, assessing accuracy, cross-validation, and Receiver Operating Characteristic (ROC) metrics. Remarkably, the proposed model achieves an accuracy value of 99.2% on the RIM-ONE DL dataset. By bridging the gap between automated diagnosis and ophthalmological practice, this research contributes significantly to the medical field. The model's robust performance and superior accuracy offer a promising avenue to support healthcare professionals in enhancing their decision-making processes, ultimately improving the quality of care for patients with retinal anomalies.

Keywords—Optic disc (OD); Optic cup (OC); U-network; restricted Boltzmann machines; squirrel search algorithm

I. INTRODUCTION

Diabetes mellitus, a common metabolic problem characterized by increased blood sugar levels, can cause diabetic retinopathy, a chronic and progressive eye condition. The retina, the light-sensitive tissue at the back of the eye in charge of conveying visual information to the brain, is especially impacted by this disorder that poses a threat to eyesight [1]. The primary cause of adult blindness globally is diabetic retinopathy, which is of great public health concern. The slow destruction of the tiny blood vessels that supply the retina is the defining feature of diabetic retinopathy. Long-term exposure to high blood glucose levels, a characteristic of diabetes, can erode and potentially harm these vulnerable blood vessels. As a result, they can start to leak, causing fluid and lipid deposits to build up in the retina. Alternately, they may narrow and reduce the retina's blood supply, causing the release of growth hormones that promote the development of aberrant blood vessels. Because these aberrant blood vessels are weak and prone to bleeding, the retina might sustain additional harm.

In order to properly manage diabetic retinopathy, early identification and prompt care are essential. Regular eye exams and specialized imaging methods, such as fundus images and optical coherence tomography (OCT), are crucial for identifying this problem and tracking its development. The development of automated methods for diabetic retinopathy screening has also been aided by developments in artificial intelligence and machine learning, which have the potential to enhance the accessibility and effectiveness of early diagnosis and treatment. Understanding and resolving the complexity of diabetic retinopathy remain crucial in preventing vision loss and raising the quality of life for people with diabetes as diabetes incidence rises internationally [2]. Recently, automated diabetic retinopathy identification using retinal

scans has shown promise thanks to machine learning. Machine learning algorithms are capable of classifying the severity of diabetic retinopathy with amazing accuracy after analysing large datasets of retinal images and extracting pertinent information. Achieving consistently excellent performance across various patient demographics and image quality situations still presents a number of obstacles. The diagnostic accuracy of traditional machine learning algorithms can be hampered by the difficulty with which complicated, hierarchical patterns in retinal images can be captured. This has motivated academics to investigate more sophisticated deep learning techniques, such as CNNs and RBMs, to improve the identification of diabetic retinopathy.

The retina was a sphere located on the retina's inner side at the eye's rear. Its purpose has been to interpret visual data using the cones and rod and other image receptors found in the eye. The macula, or retina's central region, has a black, rounded area. Sharp eyesight was provided by the macula's fovea, which is located at its centre. The body's circulatory supplies blood to the retinal cells, just like it does for any other type of tissue. Each of the veins and main arteries enter and depart the eye through the optical disc, which is formed by an optic cup. It also serves as an organ wherein the optical nerve exits the eye. The efficacy of treatments in the medical sector is increased by early illness identification. Whenever the pancreas doesn't create enough insulin, diabetes looks to be a disorder that becomes progressively. A severe public health issue, diabetes mellitus currently affects 463 million individuals globally and is expected to reach 700 million in 2045. Diabetic retinopathy (DR), a commonly prevalent eye condition associated with diabetes, affects at least 1/3rd of people who have the condition [3]. No matter how severe their diabetes has been every patient with diabetes may acquire DR, which is characterised by increasing vascular disturbances in their retinas. Non-proliferative DR (NPDR) and PDR are the two common stages of DR [3]. Among the most popular clinical measures, the International Clinical DR (ICDR) dimension, has five DR severity levels: regular, mild, serious, moderate, and excessive [4]. There has been thought to be 93 million individuals living with DR globally, making it the main causes of blindness amongst working-age individuals. These numbers are expected to rise even higher, largely as a result of rising prevalence of diabetes in emerging Asian countries like China and India [4]. Whereas the early phases of DR are typically asymptomatic, neuronal retinal injury and clinically undetectable microvascular alterations advance during this time [5]. As a result, people with diabetes should undergo routine eye exams because prompt identification and treatment of the problem are crucial [4]. Flashes and floaters, vision loss, and blurred vision have been the main signs and manifestations of DR [4]. The macula is impacted by DR, which is brought on by metabolic changes inside retinal blood cells, caused because of abnormal blood flow, and blood components and blood leaks throughout the retina. As a result, the retinal membrane swells and causes vision to become hazy or blurry. The condition damages both eyes, and with continued untreated diabetes for an extended period of time, diabetic maculopathy results in blindness [6]. Early recognition of DR has been even more crucial given that the primary preventive approach was the treatment of

hyperlipidemia, hypertension, and hyperglycemia [5]. Additionally, if diabetic maculopathy and proliferative retinopathy have been cured in the initial phases of the illness, there is a considerable reduction in the risk of blindness with currently accessible therapies, including laser imageocoagulation. It becomes clear that early identification and suitable therapy are crucial for delaying or even preventing blindness from DR [7].

With the aid of specific medically recognised and authorised comparing agents that have been inserted towards the retina, the pupil elongation occurs in order to monitor the retinal structure, including the RBVs, macula, fovea, and Optic Disc (OD). This approach makes use of a mydriatic foundation video or the fluorescein catheterization (FA). This helps to collect fundus images from people with diabetes so they may be examined for the accurate diagnosis as well as the detection of DR. Manual techniques, including bio-microscopy, fundus retinal images, Optical Coherence Tomography (OCT), Adaptive Optics, Retinal Oximetry, Scanning Laser Ophthalmoscopy (SLO), OCT Angiography, Doppler OCT, Retinal Thickness Analyzer (RTA), and many others, can be used to identify DR early on [8]. Nevertheless, the manual analysis of the disease using these traditional approaches is laborious, time-consuming, and extremely error-prone. Additionally, it necessitates an advanced task force, which is occasionally impractical given the current situation. Therefore, it is not possible to carry out manual identification for DR early identification at any moment or location. As a result, the magnitude of these difficulties has spurred extensive study and the creation of methods that instinctively analyse data and detect the DR onset. This is mainly due to the desire to lower the expense of treating the illness. The common objective of increasing the effectiveness of healthcare services has been supported by developments in medical technology [9]. e-Health structures, for instance, have been effective being employed in an assortment of healthcare routes [10], [11]. In the biomedical imaging discipline, computer vision-oriented systems are becoming more significant. They offer the radiologist valuable decision support data that improves the prognosis and effectively informs medical personnel on the optimum efficient therapies for important medical diseases. Various image modalities, including 7-field colour fundus images (CFPs), ultra-wide-field-SLO (UWF-SLO), and colour fundus images (CFIs), were employed for the evaluation and therapy of DR in the particular medical imaging realm. Benefits could include less labour for the ophthalmologist as well as a lower risk of human miscalculation. Additionally, compared to manual detection, a computerised system might be far more effective and easily able to spot lesions and anomalies. Automated of DR identification is therefore crucial. Artificial Intelligence (AI) techniques can be used to create the DR automation systems.

Development in research and innovation has improved the quality, safety, and liveability of individual life. For example, a cutting-edge field of study called automatic medical imaging assessment uses imaging technologies to spot dangerous disorders. These Computer-Aided Diagnostic (CAD) tools, also known as automatic diagnosis systems (ADSSs), offer

amenities for the benefit of people. The use of CAD systems was acknowledged in a wide range of clinical diagnoses, including the identification of brain tumours, DR, gastrointestinal problems, glaucoma, macular oedema, and many others [12]. With personal observations, such CAD technologies have generated outcomes that are comparable. The creation of CAD tools depends on the image attributes that are computationally retrieved from images [13]. Clinical staff must manually examine DR abnormalities and retinal anatomy characteristics. Furthermore, observing intra- or inter-changes in retinal elements needs technical domain expertise because human examination of DR has been subjective. As a consequence, earlier DR screening programmes with colour fundus images must be carried out by CAD technologies. Clinical staff may spend less time, money, and effort manually analysing retinal images thanks to these CAD tools [14], [15]. AI offers the ability to completely alter how eye diseases have been now diagnosed and have a profound therapeutic effect on advancing ophthalmic treatment. Prior research on automatic DR identifications has been conducted. A useful method for the automatic identification and evaluation of DR has grown up: deep analysis of fundus images. The patients in physically underserved regions where there are few ophthalmologists and scarce medical facilities could benefit from the efficient deep learning (DL) system's ability to accurately and automatically recognise more severe DR with comparable or superior reliability than learned instructors and retina experts [16].

Machine Learning (ML) is a subgroup of DL that has grown stronger and increasingly effective as a weapon. DL is also an ideal complement to ML. The DL architecture is made up of a multifaceted, hierarchical design. Classifying, segmenting, localising, and identifying medical images are major DL tasks in clinical image assessment. DL offers more promising and outstanding outcomes in the diagnosis and categorization of DR diseases using a variety of techniques. Convolutional Neural Networks (CNN), Auto encoders, Generative Adversarial Networks (GAN), Recurrent Neural Networks (RNN), Deep Boltzmann Machines (DBM), Deep Belief Networks (DBN), and Deep Neural Networks (DNN) have been a few examples of DL-based approaches. The model performs better when there has been additional training information since both low-level and high-level characteristics have been automatically retrieved and trained [17]. Convolutional Neural Networks (CNN), a fundamental framework of DL in computer-vision, have produced outstanding results with regard to forecasting and detection in the medical images categorization. By autonomously segmenting the region-of-interests (ROIs) from the initial images, DL methods streamline the feature retrieval procedure. Additionally, these methods offer a complete answer for developing and assessing the categorization model. In DL methods, The DR images have been initially gathered. The acquired DR images have been then subjected to preprocessing methods like contrast enhancement, lighting modification, and scaling to remove noisy features. After being pre-processed, those images have been sent to the DL design, which uses the learning images' distinctive characteristics as input and the retrieved attributes and their scores to acquire categorization rules. In DL training, the

attribute weights have been recursively optimised to get the optimal characteristics weight and more precisely categorise the images. These optimised weights have been finally examined on unlabelled images via a categorization layer. The use of cloud computing has permeated almost every element of human life. Cloud computing, on the other hand, has limits in terms of prolonged delays, which are detrimental to IoT activities that require real-time responses [18]. The key contribution is discussed as follows:

- The research highlights the critical importance of early diagnosis for diabetes-related retinal conditions, which can potentially lead to blindness if not identified and managed in a timely manner.
- The paper recognizes the challenges posed by labour-intensive and time-consuming traditional methods of diagnosing diabetic retinopathy and the subtlety of early glaucoma symptoms. It underscores the need for more efficient diagnostic techniques.
- The study integrates machine learning and deep learning techniques to address these challenges. Notably, the introduction of Restricted Boltzmann Machines (RBM) showcases an innovative approach to enhance the accuracy and efficiency of the diagnostic process.
- The proposed model extracts and analyses multiple features from retinal images using RBMs, facilitating the accurate categorization of anomalies. This approach holds the potential to significantly expedite the diagnostic process.
- The research further extends its impact by introducing a U-network model for optic segmentation, contributing to more precise and reliable diagnostics.
- The application of the SSA to fine-tune RBM hyper parameters demonstrates a commitment to achieving optimal model performance.
- Rigorous experimentation using the RIM-ONE DL dataset substantiates the effectiveness of the proposed methodology. The high accuracy achieved serves as a testament to the model's robustness and potential clinical relevance.
- The comprehensive comparison against previous prediction models, incorporating metrics like accuracy, cross-validation, and ROC, underscores the model's superiority in diagnostic capabilities.

The structure of this article is organized as follows: Section II reviews previous research on prediction problems using various optimization methodologies. Section III, image pre-processing improve and adjust the brightness. The OD and OC are segmented using a Threshold U-Network. Section IV discusses the rim-one-dl dataset results. Section V, experimental evaluation comprises mathematically developed system models for sensitivity, specificity, accuracy, and AUC. Section VI concludes the paper.

II. RELATED WORKS

A computer vision-based method to analyse and forecast diabetes from input retinal images was proposed by Mini Yadav et al. [19]. This facilitates the early identification of DR. Pre-processing, feature extraction, and segmentation techniques are used in the aforementioned image processing stage. Following the image processing procedures, the categorization step using ML is carried out. Python is employed for better research outcomes. For designing the coding for the empirical outcomes' platform, investigators use Jupyter. The framework created was tested on databases from open access public repositories, and it used CNN to obtain 98.50% accuracy as opposed to SVM's 87.40% accuracy. These outcomes outperform a number of sophisticated unsupervised ML approaches. It leads to a reduction in procedure complexity and enhanced evaluation metrics, making it appropriate for application in the DR detection employing retinal image assessment. The study asserts that their unsupervised ML approach outperforms previous methods, but in order to judge the robustness and generalizability of the suggested method, it must be tested on independent databases. The dependability of the outcomes might not be ensured in the absence of external testing.

The multi-scale attention network (MSA-Net) was proposed by Mohammad and Yasmine [20] for DR categorization. The suggested method uses an encoding network to place the retinal images in an upper-level representational space, enriching the representation by combining middle- and the highest-level information. The retinal morphology in a distinct locale is then described using a multi-scale characteristic hierarchy. A multi-scale attention system is added on the highest of the upper-level structure in order to improve the feature depiction's ability to discriminate. The cross-entropy loss has been employed to learn the framework in a conventional manner, and it is used to categorise the DR seriousness level. In addition, the model is instructed to distinguish between healthy and unhealthy retinal images employing the poorly annotated information. This stand-in exercise aids the model in improving its ability to distinguish between unhealthy retinal images. When used, the suggested strategy produced remarkable outcomes on the APTOS and EyePACS public databases. The study discusses the application of poorly labelled data to help the algorithm distinguish among retinal images that are healthy and those that are ill. However, if the annotations have not been precise or thorough adequate to capture the entire spectrum of abnormal retinal images, the efficacy of this method may be constrained. The training process may become biased and noisy due to insufficient annotations.

A CNN-oriented strategy was suggested by Worapan et al. [21] as a means of identifying and evaluating DR from retinal images. It could categorise the retinal images that were supplied into a normal group or atypical group that would then be automatically divided into four levels of anomalies. The suggested solution has been predicated on DeepRoot, a recently suggested CNN framework. It has one major branch and two subsidiary branches that link it. The principal feature generator for both upper- and lower-level attributes in retinal images resides in the central branch. The characteristics

produced from the central branch are then subsequently extracted by additional branches to provide more intricate and comprehensive characteristics. They use customised zoom-in/out and attenuation stratum to record the fine details of minuscule remnants of DR within retinal images. Moreover, the Kaggle database is used to train, verify and test the suggested approach. Using examples of unknown information that the researcher independently acquired from an actual circumstance in a hospital, the learned model's regularisation is assessed. Under the two categories scenario, it performs admirably, with 98.18% sensitivity. Although the research suggests evaluating the regularisation of the trained model using samples of unknowable information obtained from a healthcare facility, the specifics and extent of this verification have not been given. To guarantee that the model's performances comply with the desired purpose and to gauge its efficacy in practical contexts, rigorous real-world verification studies must be carried out in clinical settings.

Employing CNN, Raja and Balaji [22] created a reliable automated diabetic identification system for retinal images. The proposed system primarily consists of five components like preprocessing, exudates segmentation, blood vessels segmentation, extraction of textural features, and diagnosis of diabetes. The input retinal image is initially enhanced during the preprocessing stage employing adaptive histogram equalisation (AHE). As a result, fuzzy c-means clustering (FCM) and CNN have been employed for segmenting exudates and blood vessels, respectively. Following that, exudates and blood vessels are used to extract textural properties. Following extracting features, a support vector machine (SVM) is used to classify diabetic patients. The experimental findings show that, when compared to other methodologies, the suggested approach achieves improved diabetic diagnosis outcomes (sensitivity, specificity, and accuracy). To guarantee the suggested method's suitability for various populations and changes in retinal images, its efficacy and adaptability should be tested on separate databases. If various datasets were utilised to show the system's durability, the assessment should have been done on many databases, and this should be specified in the study.

The likelihood of vision loss may be considerably reduced by early diagnosis and treatment with DR. Analysis of retinal image has gained popularity as a method of disease detection in contemporary ophthalmology. Fundus angiography has been frequently used by ophthalmologists and computerised systems to find DR-based clinical indicators for DR earlier detection. Because of the imaging situations complexity, like imaging in a range of angles and lighting circumstances, fundus images are frequently exposed to inadequate contrast, sound, and inconsistent illumination problems. By lowering the noise and boosting the contrast, Saif Hameed et al. [23] proposed an algorithm for enhancing image quality that will reinforce the norm for colour fundus imaging. The method involves two primary steps: shrinking the images to eliminate extraneous information, followed by performing the shape cropping as well as gaussian smoothing to boost contrast and reduce noise. MESSIDOR and EyePACS represent two common datasets used to assess the research outcomes. It has been amply demonstrated that the findings of improved image

feature retrieval and categorization surpass those obtained without using the enhancement technique. As an IoMT usage, the updated algorithm has also been evaluated in smart hospitals. Although the research includes evaluating the revised method in smart hospitals, it is vital to take into account the practical difficulties and prerequisites for clinical deployment in the actual world. This entails integration with currently in use medical imaging equipment, regulatory authorizations, and professional acceptability. These issues should be covered in the study together with information on the difficulties and possible clinical advantages of applying the method in a clinical context.

Anas Bilal et al. [24] proposed an innovative two-stage method for automatic DR categorization. Data augmentation and pre-processing methods have been utilised to improve the image clarity and quantity because the asymmetric blood vessels (BV) and Optic Disc (OD) identification system has a low percentage of positive cases. For BV and OD segmentation during the first stage, two distinct U-Net algorithms are used. Subsequent to preprocessing for extracting and selecting the most discriminating characteristics after BV and OD extraction employing Inception-V3 depending on transfer learning (TL), the symmetrical integrated CNN-SVD framework has been developed in the secondary phase. It recognises DR by identifying retinal indicators like exudates, haemorrhages, and microaneurysms. The suggested approach displayed cutting-edge efficiency on the Messidor-2, DIARETDB0, and EyePACS-1 tests, with mean accuracy readings of 94.59 per cent, 93.52 per cent, and 97.92 per cent, correspondingly. The effectiveness of the recommended approach has been demonstrated through extensive evaluations and comparability with benchmark methods. The low affirmative case prevalence for asymmetric BV and OD recognition can make it difficult to train and assess the algorithms. The accuracy and generalizability of the suggested strategy, especially for identifying certain abnormalities connected to DR, may be impacted by the dearth of positive instances.

Phridviraj et al. [25] presented a bi-directional LSTM-oriented DR diagnosis model employing retina fundus images. The Bi-directional LSTM approach uses retinal fundus images to identify and categorise various categories of DR. The Multiscale Retinex alongside Chromaticity Preservation (MSRCP) technique is used in the suggested framework as a preprocessing stage to raise fundus image disparity and advance short discrepancy of pharmaceutical perspectives. Moreover, MSRCP is utilised to create results that are adequate for processing images. The key challenge regarding the Retinex method is setting the values for the variables, including the gain, offset, Gaussian scales, etc. Such parameters need to be altered to produce a useful result. The major objective of the presented approach is to get the ideal settings for the MSRCP procedure's variables. Additionally, an effective net-based characteristic extraction that makes of DL is used to create feature vectors from already processed images. The standard MESSIDOR database is used in numerous experiments. The outcomes are examined in light of several evaluating criteria. The findings demonstrate that the Bi-LSTM-MSRCP methodology is superior to more

contemporary techniques for DR diagnosis. Even if the research shows better results than current methods, it's crucial to take the comprehension of the suggested model into account. Since bi-directional LSTM models are frequently regarded as "black-box" models, it might be difficult to comprehend how decisions are made and the particular characteristics that contribute to DR diagnosis. The clinical acceptance and confidence in the paradigm may be constrained by its lack of comprehension.

For the purpose of DR identification, Loheswaran [26] suggested the Optimised Kernel-oriented Fuzzy C-Means (OKFCM) based Segmentation and RNN-based Categorization scheme. OD elimination and KFCM Separation performed using Modified Ant Colony Optimisation (ACO) are the two primary stages within the recommended segmentation portion. GLCM and time-built characteristics have been utilised for the grading of DR. The OKFCM-MACO-RNN was another name for the suggested framework. The OKFCM-MACO-RNN technique's sensitivity, accuracy, and specificity have values of 81.65 percent, 99.33 percent, and 99.42 percent, accordingly, have been adjusted to finish the OKFCM-MACO-RNN categorization assessment procedure in the diaretDB1 database. The OKFCM-MACO-RNN approach can be relied upon to reliably detect exudates. The OKFCM-MACO-RNN based Segmentation are evaluated with jacquard coefficient, accuracy, and dice coefficient having values of 72.84, 85.65, and 93.15 correspondingly. The quantity and variety of the database employed for learning and evaluation have a significant impact on how well the suggested framework performs. The diaretDB1 dataset has been mentioned in the study, but it is crucial to evaluate the dataset's representativeness and determine whether it effectively accounts for the variety of DR situations that are experienced in real-world circumstances. The algorithm might not work as well on other databases.

It is quite challenging to diagnose DR through laborious physical diagnosis because of the variety and complexities of DR. As a result, Spoorthi and Rekha [27] concentrated on employing an RNN-LSTM and Deep CNN (DCNN) integration to categorise a specific collection of fundus images into four phases. This method recognises all DR phases instantly. This mixture takes a lot of details from the fundus image. To create the integrated model, over 2000 fundus images have been utilised overall. This work shows that the precision of forecasting the DR phases has been greatly increased by the retrieval of those characteristics from fundus images employing RNN-LSTM and DCNN. To determine the combined model's suitability for use with various populations and changes in retinal images, its efficacy and generalizability should be examined on separate databases. To show the approach's resilience and dependability across various datasets, additional verification is required.

III. PROBLEM STATEMENT

This study focuses on improving diabetic retinopathy diagnostic accuracy and efficiency using machine learning and RBMs. Diabetic retinopathy is a major consequence of diabetes that, if not identified early, can result in blindness.

Current approaches for detecting diabetic retinopathy frequently rely on ophthalmologists doing manual assessments, which can be expensive, time-consuming, and prone to inter-observer variability. Additionally, existing automated methods sometimes have trouble recognizing retinal abnormalities with high sensitivity and specificity. The suggested strategy tries to use RBMs, a class of neural network capable of learning hierarchical representations of data, to improve the automated identification of diabetic retinopathy in order to overcome these constraints. By doing this, it hopes to provide an alternative to current techniques that is more precise, effective, and consistent [24].

However, the limits of existing diabetic retinopathy detection techniques call for improvements. First off, the diagnostic accuracy of traditional machine learning algorithms is sometimes constrained by their inability to grasp the complex patterns and subtle elements seen in retinal images. Additionally, the lack of extensive, diverse datasets for training and testing might limit the capacity of present models to generalize, particularly when faced with differences in retinal images that occur in the real world. The promise of deep learning methods like RBMs, which can build intricate, hierarchical representations from data, is also underutilized in many current approaches. The need to build a strong, RBM-based solution that can not only exceed existing approaches in terms of accuracy but also adapt successfully to changes in image quality, illness development, and patient demographics is therefore appealing.

IV. PROPOSED METHODOLOGIES

Retinal image analysis is essential to perform mass screening, even if there is a lack of experienced doctors. This work presents RBM images, the analysis uses numerous features to predict formation in images. The steps used are image acquisition, pre-processing, segmentation, and glaucoma classification. Initially, retinal fundus images are obtained from the public data source. Pre-processing is necessary to eliminate unwanted image features such as speckles, blind spots etc. The OD and OC is performed using a Threshold U-Network (Two-stage TUNet). Next, the deep features such as contrast, homogeneity, mean disc, correlation, SD (standard deviation) disc, energy disc, entropy disc,

entropy cup, SD cup, mean cup, energy cup, etc., are extracted. Fig. 1 shows flow diagram of deep learning based retinal image analysis.

A. Dataset Collection

Some confusion and incorrect usage of the three published versions prompted the proposal to update and integrate DL (rim one for deep learning), an updated version of them, was created using them. With profound learning in mind, it is designed to meet the standards mentioned earlier for the environment. The outcome of integrating the three previous versions is rim-one DL. This gives each patient and each eye a separate image. Additionally, all images were correctly cropped around the head of the optic nerve, utilizing the exact same parallelism criterion, which was not done in earlier versions.

B. Pre-Processing

Pre-processing techniques such as cropping, channel separation, and data enhancement are used to input images. A image is the removal of external parts by cropping to improve encircling, change the proportions of an angle, or emphasize a subject and resizing results in a change in its physical size. A tile is divided into the portion of data that is lost due to cropping. The original dataset contained only a limited number of images that could be used as training data. A neural network could not be applied and trained with such an amount of data. Flipping and data rotation has been used as augmentation techniques to overcome this problem. To increase the dimension of the test set, the images first had to be vertically flipped. Images are then flipped vertically, an additional increasing amount of data available. Flipped images were rotated from 0° to 180° in 20° increments after flipping. As a result, the model was effectively trained with a larger data set.

C. Segmentation of Images

The technique of splitting an image into its component sections using a segment/part of an image is known as image segmentation. The task of objects is to find a certain subdivision among the provided images. Segmentation is also used in retinal fundus images to investigate structures like the optic disc and optic cup.

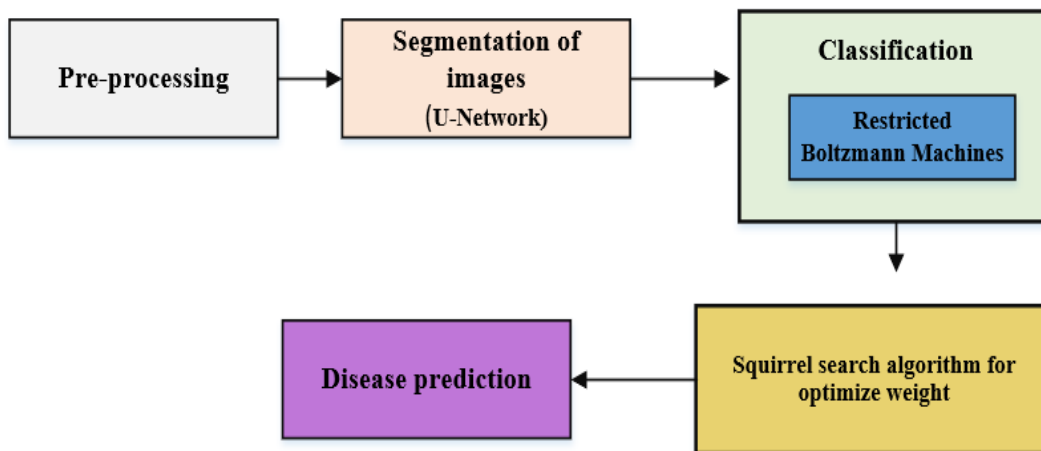


Fig. 1. Flow diagram of deep learning based retinal image analysis.

1) *OD*: The optic nerve head OD is where ganglion cells and axons leave eye to form visual cortex. If there are no shafts or cones, there is a blind zone. Because receptor rods and cones in this region are dull, the corresponding point of tiny blind spot at OD is increased. The OD is widely employed in to determine the cup-to-disc ratio.

2) *OC*: It is located in middle of the optic disc, which appears to be shaped like a white cup. The optical curve is responsible for the mobility of the retina in the human eye. The greater the distance from the optic curve's diameter, the greater the chance of developing glaucoma.

3) *Threshold U-network*: The OD and OC are segmented using a threshold U-network (TUNet). During processing, both OD and OC segmentation are two-stage thresholds [28]. A fundamental image processing approach is threshold segmentation. Varying tissues in medical imaging are often displayed at different levels of intensity. The threshold eliminates the uninteresting areas while also reducing noise interference. This process is both required and efficient. The threshold value must be chosen carefully. The region of interest will be impacted if the threshold range is too tiny; as a result, the experimental results are inaccurate. Noise reduction becomes difficult if the threshold range is set too high. The threshold range is often defined by experience. The two-stage U-Net design is used for the threshold interval computations. As glaucoma detection must be divided into two groups, it is challenging to segregate glaucoma data in real time (OD and

OC).To simplify and reduce the complexity of the problem, a two-stage U-Net framework is used and composed of total glaucoma segmentation and glaucoma substructure segmentation (the second step). The primary goal of the U-net architecture is the segmentation of the many substructures of the system [29]. Fig. 2 illustrates the U-Net framework.

D. Restricted Boltzmann Machines (RBM) Diabetic Retinopathy Classification

Using input vector f , concealed units s , weights matrices C , visible biases y , plus hidden biases z as shown, the RBM may be shown as a graph that is undirected.

$$L(s = 1|f) = \sigma(z + C.f)$$

$$L(f = 1|s) = \sigma(y + C.s) \tag{1}$$

The binary data acquired by applying the CLBP descriptors is transformed into actual value matrices in our process using RBMs. This information comprises image characteristics which the first set of CNN filters that have been trained under supervision often recognise, such as edges, blobs, or basic forms. Utilising RBMs enables bypassing these layers, leading to a reduced architecture to address a particular image categorization job. As a result, we are able to analyse more complicated features in the initial convolutional layers thanks to our prior processing and the RBM layers. Fig. 4 shows the restricted Boltzmann machine.

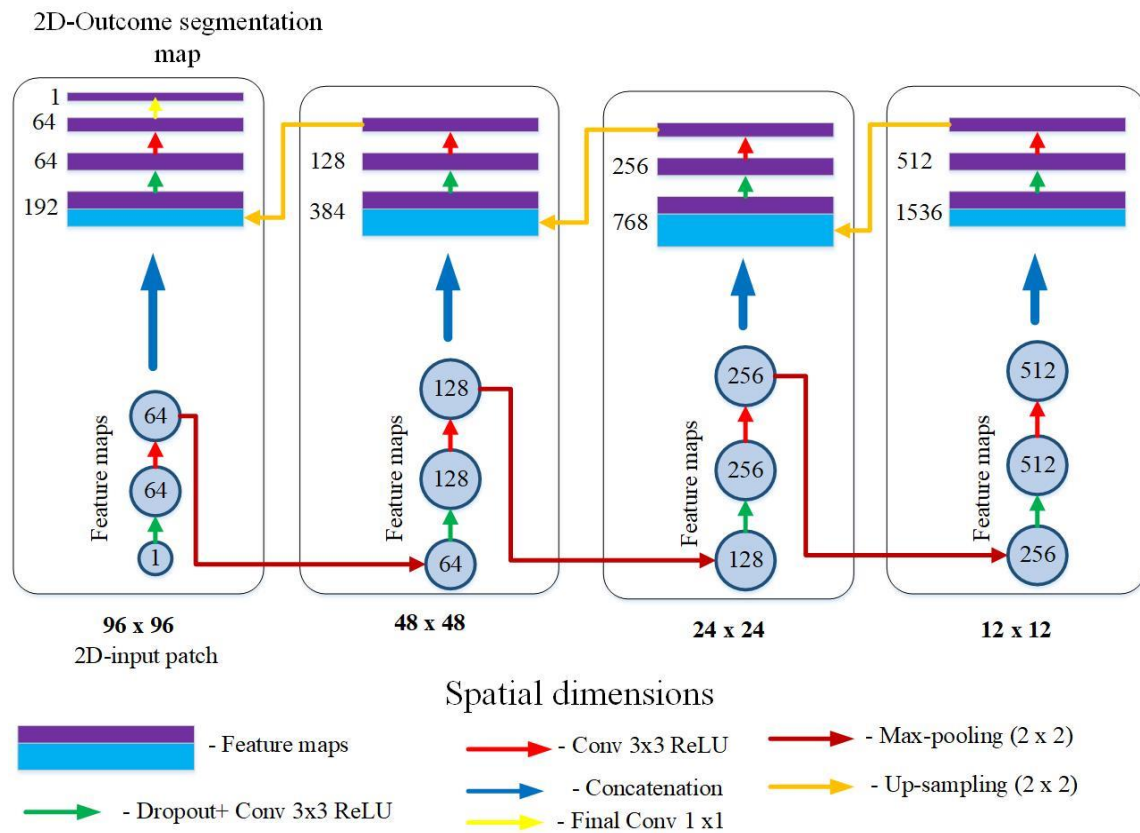


Fig. 2. U-net architecture.

The RBM analyses the information once the CLBP step is complete. The total amount of observable subunits is 16 in the most basic version since descriptor values are supplied immediately to the RBM, and bigger receptivity areas are possible by combining CLBP characteristics from a kernel of size P. The dimension of an output matrix as well as the overlapping sections may be modified using the stride length G. The RBM output vector v has a length of $m = P^2$.

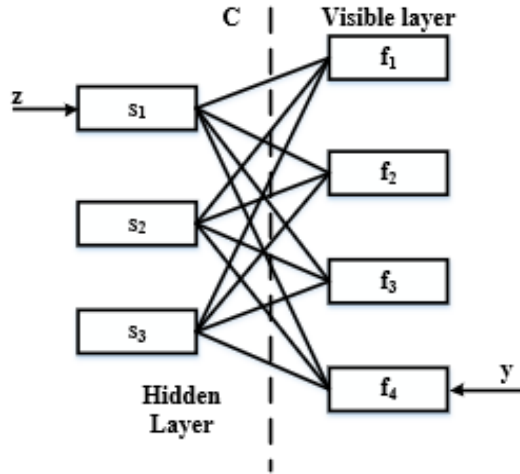


Fig. 3. Illustration of a restricted Boltzmann machine.

The input vector for the RBM is shown in Fig. 3 being created for $P = 2$. The RBM layer's feed is a matrix created as following.

$$RBM_{1/P} = \begin{bmatrix} f(1,1) & f(1,2) & \dots & f(1,m) \\ f(2,1) & f(2,2) & \dots & f(2,m) \\ \vdots & \vdots & \vdots & \vdots \\ f(m,1) & f(m,2) & \dots & f(m,m) \end{bmatrix} \quad (2)$$

The numerical value within the s_i component corresponding to the accessible vector f is given by because the RBM in this design de facto transforms into a typical neural network feeding forward with the activation function of sigmoid.

$$s_i = \sigma(z_i + \sum_j c_{ji} f_j) \quad (3)$$

In matrices recording, the final solution that describes the RBM level is

$$\sigma(Z + C \cdot RBM_{1/P}) \quad (4)$$

The scope that the vector produced by the preparation workflow relies on the number of hidden elements (RH) or cadence (S), which determines how multidimensional the resulting data is,

$$\left[\frac{C}{G} \times \frac{S}{G} \times RH \right] \quad (5)$$

wherein, the supplied image's parameters are $[C \times S]$. The whole pretreatment workflow and the CLBP-RBM translation are shown in Fig. 4.

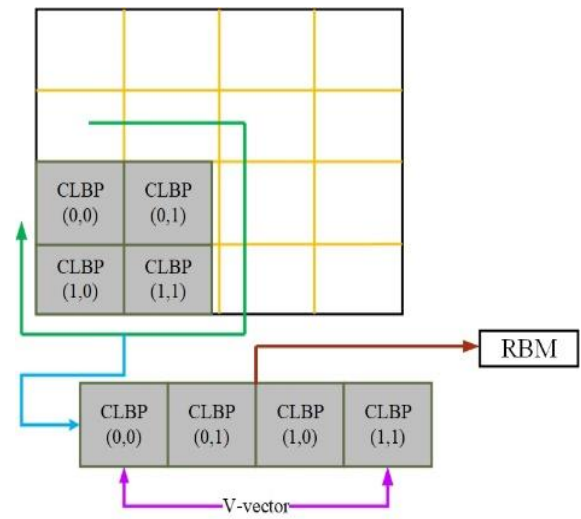


Fig. 4. CLBP kernels.

1) *Squirrel search algorithm for weight optimization*: The proposed method has 2 search methods: the first is jumping method, and second is a broadminded method. As part of evolutionary process, the practical method is automatically selected through the selection strategy of linear regression, which increases the robustness of a squirrel search algorithm. The escape process sufficiently creates a searching area, and the demise procedure uses the leaping mechanism in order to examine the created space. The capacity of SSA to evolve and explore is balanced. Regarding the incremental search approach, mutations operation maintains the present historical data and gives greater consideration to maintaining population diversity.

a) *Random initialization*: Initial population W was generated randomly with k number of flying squirrels.

$$W = \begin{bmatrix} W_{1,1} & W_{1,2} & \dots & \dots & W_{1,d} \\ W_{2,1} & W_{2,2} & \dots & \dots & W_{2,d} \\ \vdots & \vdots & \vdots & \vdots & \vdots \\ \vdots & \vdots & \vdots & \vdots & \vdots \\ W_{m,1} & W_{m,2} & \dots & \dots & W_{m,d} \end{bmatrix} \quad (6)$$

In this case, $W_{i,j}$ indicates the j^{th} dimension of i^{th} flying squirrel. In a forest, flying squirrels are allocated their initial locations according to a uniform distribution.

$$W_i = W_L + U(0,1) \times (W_U - W_L) \quad (7)$$

A distributed uniformly random number in the range $[0, 1]$ is $U(0,1)$, and W_L and W_U represent lower and upper bounds for j^{th} dimension i^{th} flying squirrel.

b) *Fitness evaluation*: To calculate the localization, fitness values of the defined by users fitness coefficient has choice parameters (solution vectors) placed into it. The following table contains the values that were obtained:

$$f = \begin{bmatrix} f(|W_{1,1}, W_{1,2}, \dots, W_{1,d}|) \\ f(|W_{2,1}, W_{2,2}, \dots, W_{2,d}|) \\ \vdots \\ f(|W_{n,1}, W_{n,2}, \dots, W_{n,d}|) \end{bmatrix} \quad (8)$$

The value of fitness neural network layer weight depicts the quality of optimal weight. Here $W = (w_t^c, w_t^{cap}, w_t^{GRU})$, after storing the fitness values, array is sorted in ascending order. The squirrel with a minimum chestnut nut tree declares itself to have a fitness value. Afterwards, best three flying squirrels are thought to move to hickory nut trees from acorn trees.

c) *Generating location:*

Case 1: Hovering squirrels may move from acorn nut trees $(W_{i,j})_{ant}$ to hickory nut trees $(W_{i,j})_{hnt}$. It is possible to determine the new location of squirrels in this case by following these steps:

$$(W_{i,j})_{ant} = \begin{cases} (W_{i,j})_{ant} + x_g \times s_c \times ((W_{i,j})_{hnt} - (W_{i,j})_{ant}) & \text{if } R_1 \geq P \\ \text{random location} & \text{otherwise} \end{cases} \quad (9)$$

Where x_g indicates a distance of random gliding, R_1 indicates a random number in range of [0,1], $(W_{i,j})_{hnt}$ denotes location of squirrel reached hickory nut tree and t represent current iteration. In mathematical model, the gliding constant s_c is used with the purpose of striking a balance amid exploration and extraction.

Case 2: A squirrel on a normal tree $(W_{i,j})_{nort}$ can move towards an acorn tree; new location of the squirrel can be determined as follows:

$$(W_{i,j})_{nort} = \begin{cases} (W_{i,j})_{nort} + x_g \times s_c \times ((W_{i,j})_{ant} - (W_{i,j})_{nort}) & \text{if } R_2 \geq P \\ \text{random location} & \text{otherwise} \end{cases} \quad (10)$$

Case 3: In some cases, squirrels that have already consumed acorns on normal trees may settle in hickory trees to stockpile beech nuts which might be eaten during famine. Thus, the following information may be used to find new squirrel locations:

$$(W_{i,j})_{nort} = \begin{cases} (W_{i,j})_{nort} + x_g \times s_c \times ((W_{i,j})_{hnt} - (W_{i,j})_{nort}) & \text{if } R_3 \geq P \\ \text{random location} & \text{otherwise} \end{cases} \quad (11)$$

In this case, R_3 represents a random number in the range of [0, 1]. The optimization algorithm was designed using an approximated model of the gliding behaviour. Flying squirrel fitness values are computed, and the locations are updated on

each iteration until the maximum number of iterations is reached.

V. RESULT AND DISCUSSION

The experimental setup, performance measurement, evaluation datasets, and experimental outcomes are all described in this section. The discussion of the results includes an evaluation of the proposed SSA algorithm. OD and OC were trained with the original data and merged with the image to demonstrate the effectiveness of the system based on deep feature extraction and classification.

A. *Simulation Environment*

Evaluate the proposed early-stage glaucoma disease prediction technique using the Python software in a simulated environment utilizing rim-one-dl datasets. The test is run on a machine equipped with an Intel(R) Core (TM) i5 CPU @ 3200 Mhz, 3 core(s), 4 logical pro. And micro software 10 pro, a micro soft corporation, is an OS manufacturer installed physical memory (RAM) 8GM. Table I shows simulation parameters for the rim-one-dl datasets.

TABLE I. SIMULATION PARAMETERS OF BOTH DATASETS

Simulation parameters for Rim-one-dl	Values
Batch size	2
Epoch	100
Activation function	Sigmoid
Dropout	0.5
Kernel size	(3,3)

B. *Performance Evaluation*

Fig. 5 compares the accuracy plot of the proposed ensemble DeepNet with conventional pre-trained models such as CapsNet, VGG 16 and DenseNet for the rim-one-dl datasets. An epoch in artificial neural networks is one loop that covers the whole training dataset. Training a neural network typically takes many epochs. The plot of CapsNet, shows a larger difference between validation and training accuracy. This shows that the model may be overfitted. Furthermore, the improvement in accuracy has not been constant. There are substantial gaps between training and validation at a few epochs. Furthermore, the training accuracy is significantly lower at the last epoch than the validation accuracy.

Furthermore, in the DenseNet plots in figures, the training accuracy is higher than the validation accuracy. This indicates that the model is overfitting, and the peaks are not increasing consistently. The training accuracy of DenseNet is continually rising; however, the validation accuracy is not. There is also a decrease in validation accuracy after a few epochs, which is undesirable. As a result, the model underperforms and is unsuitable for predicting abnormality.

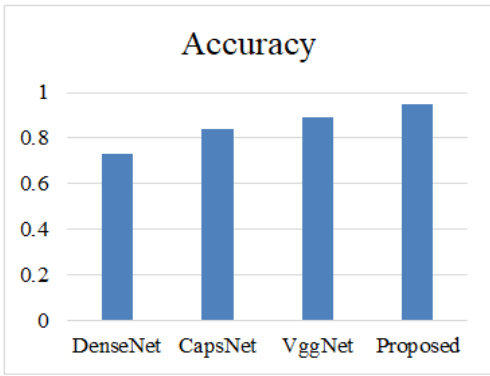


Fig. 5. (a) Accuracy plot.

Fig. 6 depicts the overall performance of several criteria, such as accuracy, specificity, recall, and precision, using the rim-one-dl datasets. It is based on deepnet ensembles such as deep CNN with multi-pooling layer, dual part scaled cross dense network, and graph CapsNet. Accurate is the ratio of correct predictions to the total prediction or true value. It is usually multiplied by 100 to express it as a percentage. It quantifies the accuracy of the classifier model and is scientifically calculated as

$$accuracy = \frac{TP + TN}{P + N} = \frac{TP + TN}{TP + TN + FP + FN} \quad (12)$$

Where TP denotes True positive, TN denotes True negative, FP denotes false positive and FN denotes false negative. Fig. 6 clearly shows that the proposed one provides the highest accuracy, which is determined to be the rim-one-dl dataset. In contrast, other classifiers provide significantly lower accuracy. In terms of specificity, it again takes the lead regarding values compared to other classifiers. In the KGD dataset, the Capsnet is found to provide an accuracy that is somewhat close to the designed accuracy. CapsNet is an ANN machine learning system that may be used to better simulate hierarchical connections. CapsNet’s slow training and testing, lacks of spatial information is its drawback. As a result, its performance is reduced compared to the proposed model.

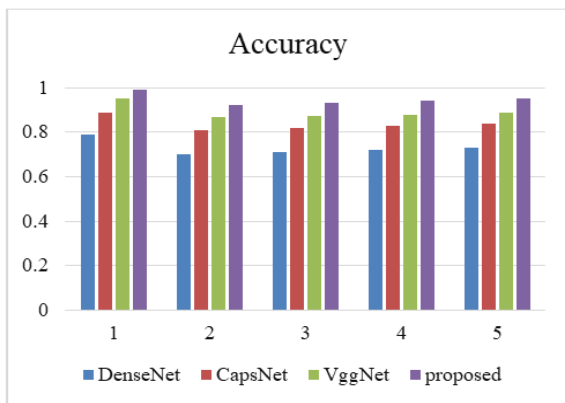


Fig. 6. Comparison graph for accuracy.

Also, a DenseNet is a convolutional neural network that uses dense connections between layers through Dense Blocks, which connect all levels directly. Each layer’s DenseNet feature maps are spliced with the previous layer, and the data is copied numerous times. However, the existing dense blocks did not consider the hierarchical features or concatenate the hierarchical features merely without removing the redundant features. As a result, its performance is not high as possible. The VGG16 network is large, implying it takes longer to train its parameters. Also, using the Max pooling layer in VGG16 caused information loss. The proposed model has tackled these issues using multi pooling layer, dual-part scaled cross-dense block and graph CapsNet. Hence, the proposed ensemble model outperforms all the pre-trained models shows in Fig. 6.

The rim-one-dl dataset utilized in the proposed research is one example of a dataset with varied comparison results that might vary due to a number of circumstances. The intrinsic diversity of data properties among datasets, including changes in image quality, resolution, noise levels, and the occurrence of certain retinal disorders, is a significant determining factor. Additionally, the design and training methods of the suggested algorithms might affect how well they function, which can make them more effective at managing particular kinds of data. On datasets with related features, algorithms designed for particular data qualities, such as those optimized for high-resolution retinal scans or skilled at managing noisy datasets, may perform better. Conversely, when applied to datasets with diverse properties, algorithms that lack the capacity to adapt to individual data changes may function inconsistently or with lower efficacy. The accuracy and generalizability of diabetic retinopathy detection systems can be enhanced by better understanding the specifics of each dataset and optimizing algorithms in accordance with those details.

The Jaccard Index is a statistical metric used to compare the similarity of samples. It is commonly referred to as the “Crossroads above the Union”. The Jaccard Index is the ratio of the intersection’s size to the samples’ union. It can have a minimum value of “0” and a maximum value of “1”. It is described mathematically as follows:

$$jaccard\ index, J(Gr, Sg) = \frac{Gr \cap Sg}{Gr \cup Sg} \quad (13)$$



Fig. 7. Segmentation performance.

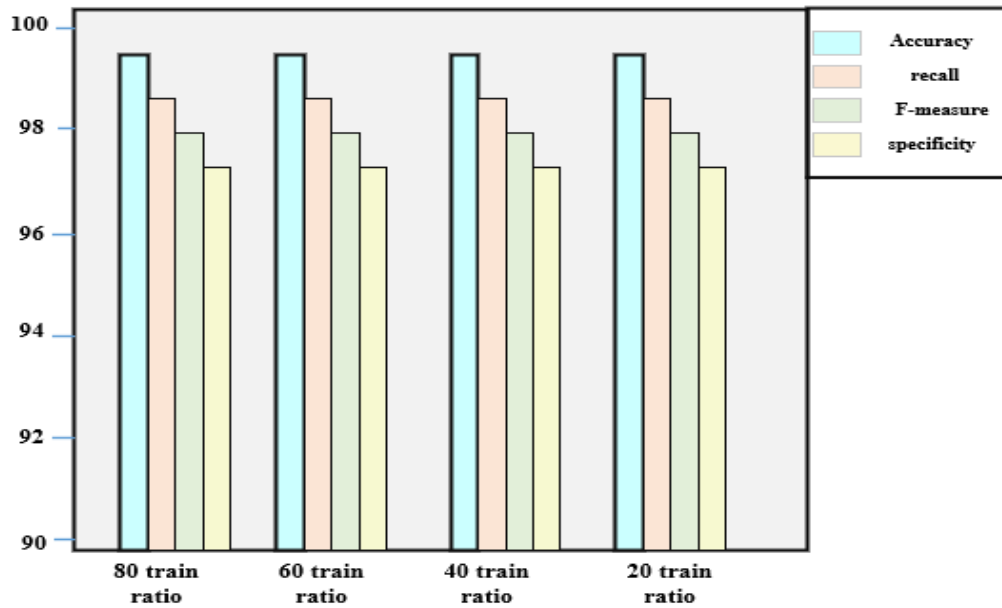


Fig. 8. Cross validation graph.

The k-fold cross-validation approach has several variants. The following are regularly used variants: Training and testing split: In the extreme, k can be set to 2 (rather than 1), resulting in a single train/test split for model evaluation. The cross validation for the rim-one-dl dataset and the KGD dataset is shown in the above Fig. 7. A typical procedure for testing the performance of a k-fold cross-validation model is the entire data set is randomly divided into independent k-folds without replacement. Fig. 8 shows the cross validation graph.

ROC curves in Fig. 9 were displayed to visually evaluate ensemble approaches based on the association between true positive and false positive rates for each deepNet. The graph shows better outcomes when such a curve is closer to the top-left corner. Using the rim-one-dl, the AUC value outperforms the existing Deepnet CapsNet, DenseNet, and VGG16. As a baseline, a random classifier is expected to give points along the diagonal (FPR = TPR). Below Fig. 9 shows the ROC curves of ensemble methods using deep CNN with multi pooling layer, dual part scaled cross dense network, and graph CapsNet.

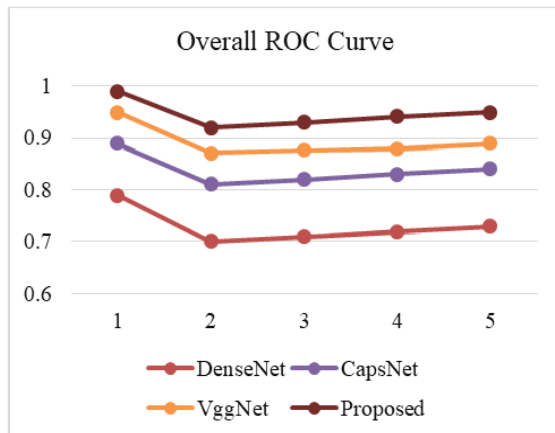


Fig. 9. ROC graph.

Plateaus or occasional dips might indicate challenges or local optima. Overall, the graph provides insight into the optimization's progress and efficiency in enhancing the solution's fitness over successive iterations.

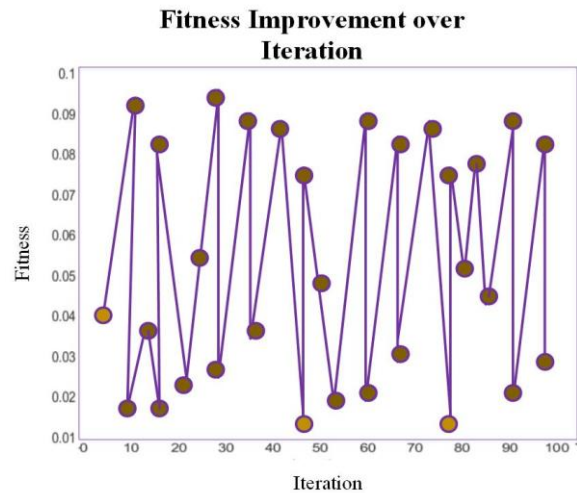


Fig. 10. Fitness improvement graph.

Above Fig. 10 illustrates how a certain fitness metric evolves across multiple iterations of an optimization process. The x-axis represents the iterations or time steps, while the y-axis represents the fitness metric. The graph demonstrates how the fitness value changes as the optimization algorithm refines its solution. Generally, the graph shows an initial steep improvement as the algorithm quickly converges towards better solutions, followed by a gradual slope as further improvements become harder to achieve.

C. Discussion

When compared to current techniques, the suggested method shows a lot of potential for the identification of

diabetic retinopathy. Traditional methods, which frequently rely on ophthalmologists' manual evaluation or crude automated algorithms, can be time-consuming, prone to human error, and unscalable in light of the expanding prevalence of diabetes worldwide. Contrarily, using the strength of RBMs is a state-of-the-art innovation that enables the automatic extraction of complex, hierarchical information from retinal images. This deep learning method offers a robust solution that can adapt to a variety of patient demographics and varied image quality situations, with the potential to significantly improve the accuracy and efficacy of diagnosing diabetic retinopathy. This suggested method, which uses RBMs, not only performs better than current methods but also represents a substantial advance in the early and accurate diagnosis of diabetic retinopathy, thereby assisting in the preservation of eyesight and the efficient use of healthcare resources.

VI. CONCLUSION

In conclusion, this research presents a promising approach for automated diagnosis of diabetic retinopathy using restricted Boltzmann machines (RBMs) and retinal fundus images (RFIs). The proposed model incorporates various elements of prediction in retinal images, with a particular focus on the segmentation of using a thresholds U-network model. This segmentation step is crucial for identifying specific regions of interest in the retinal images and enables the subsequent classification process. To optimize the performance of the RBM, the research employs the Squirrel search algorithm (SSA) for selecting optimal hyperparameters and minimizing the weight of the RBM. The use of SSA helps improve the overall accuracy and efficiency of the automated diagnosis system. The evaluation of the model on the Rimone-dl dataset showcases promising results, achieving an accuracy of 99.2%. This high level of accuracy demonstrates the potential of the proposed system in accurately categorizing anomalies and aiding ophthalmologists in early and precise prediction of diabetic retinopathy. Future research may look at the integration of deep learning architectures, like CNNs, to increase feature extraction from retinal images and better classification accuracy for improving diabetic retinopathy diagnosis using machine learning using Restricted Boltzmann Machines. An interesting research direction may also involve investigating the possibility of federated learning and transfer learning techniques to use large-scale, heterogeneous datasets for better model generalisation in actual clinical scenarios.

REFERENCES

- [1] U. Ishtiaq, S. Abdul Kareem, E. R. M. F. Abdullah, G. Mujtaba, R. Jahangir, and H. Y. Ghafoor, "Diabetic retinopathy detection through artificial intelligent techniques: a review and open issues," *Multimed. Tools Appl.*, vol. 79, no. 21–22, pp. 15209–15252, Jun. 2020, doi: 10.1007/s11042-018-7044-8.
- [2] W. L. Alyoubi, W. M. Shalash, and M. F. Abulkhair, "Diabetic retinopathy detection through deep learning techniques: A review," *Inform. Med. Unlocked*, vol. 20, p. 100377, 2020, doi: 10.1016/j.imu.2020.100377.
- [3] A. J. Jenkins, M. V. Joglekar, A. A. Hardikar, A. C. Keech, D. N. O'Neal, and A. S. Januszewski, "Biomarkers in Diabetic Retinopathy," *Rev. Diabet. Stud.*, vol. 12, no. 1–2, pp. 159–195, 2015, doi: 10.1900/RDS.2015.12.159.
- [4] N. Tsiknakis et al., "Deep learning for diabetic retinopathy detection and classification based on fundus images: A review," *Comput. Biol. Med.*, vol. 135, p. 104599, Aug. 2021, doi: 10.1016/j.combiomed.2021.104599.
- [5] H. Safi, S. Safi, A. Hafezi-Moghadam, and H. Ahmadi, "Early detection of diabetic retinopathy," *Surv. Ophthalmol.*, vol. 63, no. 5, pp. 601–608, Sep. 2018, doi: 10.1016/j.survophthal.2018.04.003.
- [6] J. P. Medhi and S. Dandapat, "An effective fovea detection and automatic assessment of diabetic maculopathy in color fundus images," *Comput. Biol. Med.*, vol. 74, pp. 30–44, Jul. 2016, doi: 10.1016/j.combiomed.2016.04.007.
- [7] L. Hill and L. E. Makaroff, "Early detection and timely treatment can prevent or delay diabetic retinopathy," *Diabetes Res. Clin. Pract.*, vol. 120, pp. 241–243, Oct. 2016, doi: 10.1016/j.diabres.2016.09.004.
- [8] J. K. H. Goh, C. Y. Cheung, S. S. Sim, P. C. Tan, G. S. W. Tan, and T. Y. Wong, "Retinal Imaging Techniques for Diabetic Retinopathy Screening," *J. Diabetes Sci. Technol.*, vol. 10, no. 2, pp. 282–294, Mar. 2016, doi: 10.1177/1932296816629491.
- [9] M. W. Nadeem et al., "Brain Tumor Analysis Empowered with Deep Learning: A Review, Taxonomy, and Future Challenges," *Brain Sci.*, vol. 10, no. 2, p. 118, Feb. 2020, doi: 10.3390/brainsci10020118.
- [10] M. Anam et al., "Osteoporosis Prediction for Trabecular Bone using Machine Learning: A Review," *Comput. Mater. Contin.*, vol. 67, no. 1, pp. 89–105, 2021, doi: 10.32604/cmc.2021.013159.
- [11] M. W. Nadeem, H. G. Goh, A. Ali, M. Hussain, M. A. Khan, and V. A. Ponnusamy, "Bone Age Assessment Empowered with Deep Learning: A Survey, Open Research Challenges and Future Directions," *Diagnostics*, vol. 10, no. 10, p. 781, Oct. 2020, doi: 10.3390/diagnostics10100781.
- [12] M. I. Razzak, S. Naz, and A. Zaib, "Deep Learning for Medical Image Processing: Overview, Challenges and the Future," in *Lecture Notes in Computational Vision and Biomechanics*, vol. 26. Cham: Springer International Publishing, 2018, pp. 323–350. doi: 10.1007/978-3-319-65981-7_12.
- [13] K. Xu, D. Feng, and H. Mi, "Deep Convolutional Neural Network-Based Early Automated Detection of Diabetic Retinopathy Using Fundus Image," *Molecules*, vol. 22, no. 12, p. 2054, Nov. 2017, doi: 10.3390/molecules22122054.
- [14] S. Keel, J. Wu, P. Y. Lee, J. Scheetz, and M. He, "Visualizing Deep Learning Models for the Detection of Referable Diabetic Retinopathy and Glaucoma," *JAMA Ophthalmol.*, vol. 137, no. 3, p. 288, Mar. 2019, doi: 10.1001/jamaophthalmol.2018.6035.
- [15] F. Zabihollahy, A. Lochbihler, and E. Ukwatta, "Deep learning based approach for fully automated detection and segmentation of hard exudate from retinal images," in *Medical Imaging 2019: Biomedical Applications in Molecular, Structural, and Functional Imaging*, B. Gimi and A. Krol, Eds., San Diego, United States: SPIE, Mar. 2019, p. 7. doi: 10.1117/12.2513034.
- [16] S.-I. Pao, H.-Z. Lin, K.-H. Chien, M.-C. Tai, J.-T. Chen, and G.-M. Lin, "Detection of Diabetic Retinopathy Using Bichannel Convolutional Neural Network," *J. Ophthalmol.*, vol. 2020, pp. 1–7, Jun. 2020, doi: 10.1155/2020/9139713.
- [17] V. S and V. R, "A Survey on Diabetic Retinopathy Disease Detection and Classification using Deep Learning Techniques," in *2021 Seventh International conference on Bio Signals, Images, and Instrumentation (ICBSII)*, Chennai, India: IEEE, Mar. 2021, pp. 1–4. doi: 10.1109/ICBSII51839.2021.9445163.
- [18] A. Elhadad, F. Alanazi, A. I. Taloba, and A. Abozeid, "Fog Computing Service in the Healthcare Monitoring System for Managing the Real-Time Notification," *J. Healthc. Eng.*, vol. 2022, pp. 1–11, Mar. 2022, doi: 10.1155/2022/5337733.
- [19] M. Yadav, R. Goel, and D. Rajeswari, "A Deep Learning Based Diabetic Retinopathy Detection from Retinal Images," in *2021 International Conference on Intelligent Technologies (CONIT)*, Hubli, India: IEEE, Jun. 2021, pp. 1–5. doi: 10.1109/CONIT51480.2021.9498502.
- [20] M. T. Al-Antary and Y. Arafa, "Multi-Scale Attention Network for Diabetic Retinopathy Classification," *IEEE Access*, vol. 9, pp. 54190–54200, 2021, doi: 10.1109/ACCESS.2021.3070685.

- [21] W. Kusakunniran et al., "Detecting and staging diabetic retinopathy in retinal images using multi-branch CNN," *Appl. Comput. Inform.*, Dec. 2022, doi: 10.1108/ACI-06-2022-0150.
- [22] C. Raja and L. Balaji, "An Automatic Detection of Blood Vessel in Retinal Images Using Convolution Neural Network for Diabetic Retinopathy Detection," *Pattern Recognit. Image Anal.*, vol. 29, no. 3, pp. 533–545, Jul. 2019, doi: 10.1134/S1054661819030180.
- [23] S. H. Abbood, H. N. A. Hamed, M. S. M. Rahim, A. Rehman, T. Saba, and S. A. Bahaj, "Hybrid Retinal Image Enhancement Algorithm for Diabetic Retinopathy Diagnostic Using Deep Learning Model," *IEEE Access*, vol. 10, pp. 73079–73086, 2022, doi: 10.1109/ACCESS.2022.3189374.
- [24] A. Bilal, L. Zhu, A. Deng, H. Lu, and N. Wu, "AI-Based Automatic Detection and Classification of Diabetic Retinopathy Using U-Net and Deep Learning," *Symmetry*, vol. 14, no. 7, p. 1427, Jul. 2022, doi: 10.3390/sym14071427.
- [25] M. S. B. Phridviraj, R. Bhukya, S. Madugula, A. Manjula, S. Vodithala, and M. S. Waseem, "A bi-directional Long Short-Term Memory-based Diabetic Retinopathy detection model using retinal fundus images," *Healthc. Anal.*, vol. 3, p. 100174, Nov. 2023, doi: 10.1016/j.health.2023.100174.
- [26] K. Loheswaran, "Optimized KFCM Segmentation and RNN Based Classification System for Diabetic Retinopathy Detection," in *ICCCE 2020*, A. Kumar and S. Mozar, Eds., in *Lecture Notes in Electrical Engineering*, vol. 698. Singapore: Springer Nature Singapore, 2021, pp. 1309–1322. doi: 10.1007/978-981-15-7961-5_119.
- [27] K. V. Spoorthi and B. S. Rekha, "Diabetic Retinopathy Prediction using Deep learning," in *2021 IEEE International Conference on Computation System and Information Technology for Sustainable Solutions (CSITSS)*, Bangalore, India: IEEE, Dec. 2021, pp. 1–6. doi: 10.1109/CSITSS54238.2021.9683553.
- [28] A. Chakravarty and J. Sivswamy, "A Deep Learning based Joint Segmentation and Classification Framework for Glaucoma Assesment in Retinal Color Fundus Images," 2018, doi: 10.48550/ARXIV.1808.01355.
- [29] T. Liu, Y. Tian, S. Zhao, X. Huang, and Q. Wang, "Automatic Whole Heart Segmentation Using a Two-Stage U-Net Framework and an Adaptive Threshold Window," *IEEE Access*, vol. 7, pp. 83628–83636, 2019, doi: 10.1109/ACCESS.2019.2923318.